

Med12 is essential for early mouse development and for canonical Wnt and Wnt/PCP signaling

Pedro P. Rocha^{1,2,3}, Manuela Scholze^{1,2}, Wilfrid Bleiß⁴ and Heinrich Schrewe^{1,2,*}

SUMMARY

The Mediator complex is commonly seen as a molecular bridge that connects DNA-bound transcription factors to the RNA polymerase II (Pol II) machinery. It is a large complex of 30 subunits that is present in all eukaryotes. The Med12 subunit has been implicated not only in the regulation of Pol II activity, but also in the binding of transcription factors to the bulk of the Mediator complex. We targeted *Med12* in mouse embryonic stem cells to investigate the in vivo function of this subunit. We report here the developmental defects of *Med12* hypomorphic mutants that have a drastic reduction in Med12 protein levels. These mutants fail to develop beyond embryonic day 10 and have severe defects in neural tube closure, axis elongation, somitogenesis and heart formation. We show that in *Med12* hypomorphic embryos, the Wnt/planar cell polarity pathway is disrupted and that canonical Wnt/ β -catenin signaling is impaired. In agreement with this, embryos that are incapable of Med12 expression failed to establish the anterior visceral endoderm or activate brachyury expression, and did not complete gastrulation.

KEY WORDS: Gastrulation, Mediator, Neural tube closure, Planar cell polarity, Somitogenesis, Wnt signaling, Mouse

INTRODUCTION

The Mediator, which is a large protein complex of 30 subunits, is a component of the intricate mechanisms that regulate eukaryotic transcription and thereby control organism development and homeostasis (Bourbon et al., 2004; Taatjes et al., 2004). It conveys information from DNA-binding transcription factors to RNA polymerase II (Pol II) and general transcription factors. As an essential coordinator for transcriptional regulation, the Mediator complex is responsible for integrating different signaling events into the appropriate response at the level of RNA transcription and can be recruited either for transcriptional activation or repression (Conaway et al., 2005; Malik and Roeder, 2005). The Mediator is conserved in all eukaryotic organisms, and in yeast it is required for the transcription of almost all genes (Bourbon, 2008; Takagi and Kornberg, 2006).

Subunits that are thought to be necessary for all functions of the Mediator, such as for interaction with the Pol II machinery or scaffold maintenance of the complex, have been shown to be essential for cell survival (Tudor et al., 1999; Westerling et al., 2007). For some subunits, however, deficiencies can be linked to a lack of signaling from specific transcription factors. For example, Med1 has been shown to be responsible for connecting transcription factors of the nuclear receptor superfamily to the Mediator complex, and *Med1*-null embryos die at embryonic day 11 (E11) due to cardiac abnormalities and placental defects (Ito et al., 2000).

Med12 has been linked to general functions of the complex and to specific interactions with transcription factors. It is part of the Cdk8 module of the Mediator, together with Med13, Cdk8 and CycC (Ccnc – Mouse Genome Informatics). This module interacts

transiently with the other components of the Mediator and a role as a negative regulator was originally proposed (Akoulitchev et al., 2000; Elmlund et al., 2006). It was recently shown that, together with Med13, Med12 can lead to transcriptional repression independently of the kinase activity of Cdk8 (Knuesel et al., 2009). Other reports have shown that, under specific circumstances, the Cdk8 module can also act as a positive co-regulator (Donner et al., 2007).

Zebrafish models have shown that Med12 is required for gene-specific functions during development, implicating Med12 also as a co-regulator of specific transcription factors. Various *med12* zebrafish mutants have been described, showing defects in neural crest formation, chondrogenesis and organogenesis of the brain, liver, pancreas and kidney (Hong et al., 2005; Rau et al., 2006; Shin et al., 2008; Wang et al., 2006). Some of these phenotypes can be explained by failure in the activation of target genes by transcription factors such as Sox9, Sox32 and Foxa2. The role of MED12 as a coactivator for SOX9 has also been confirmed in human cells (Zhou et al., 2002). Other interactors include Gli3, an effector of the sonic hedgehog (Shh) signaling pathway, which uses Med12 as a partner for repression of its target genes, and β -catenin, which requires Med12 for transcriptional activation in response to Wnt signals (Kim et al., 2006; Zhou et al., 2006). Additionally, Med12 interacts with G9a (Ehmt2 – Mouse Genome Informatics), a histone methyl transferase that is responsible for transcriptionally repressive H3K9 mono- and di-methylation (Ding et al., 2008).

Since no mouse model is available for Med12, it is not yet clear whether its developmental functions as described in zebrafish are conserved in mammals. To elucidate whether specific signaling pathways rely on Med12 to recruit the Mediator complex or whether Med12 is actually required in a more general fashion to regulate transcription, we generated such a mouse model. We targeted the X-chromosome-linked *Med12* gene in mouse embryonic stem (ES) cells and generated a hypomorphic and a null allele. The developmental defects of both these models show that Med12 is required for gene-specific functions during mouse development and that it is necessary for correct Wnt/ β -catenin and Wnt/planar cell polarity (PCP) signaling.

¹Institute of Medical Genetics, Charité-University Medicine Berlin, Berlin 12200, Germany. ²Department of Developmental Genetics, Max-Planck Institute for Molecular Genetics, 14195 Berlin, Germany. ³Faculty of Biology, Free University Berlin, 14195 Berlin, Germany. ⁴Department of Molecular Parasitology, Humboldt-University Berlin, 10115 Berlin, Germany.

* Author for correspondence (schrewe@molgen.mpg.de)

MATERIALS AND METHODS

Generation of *Med12* mutant mice

G4 ES cells (George et al., 2007) were used for *Med12* targeting. Clones that had undergone homologous recombination were identified by Southern blot analysis using a probe located outside the 3' homology region. Mouse genotyping was carried out by PCR analysis using the following primer pair: P1, 5'-AGGCACCGAGTACCTGTTCAAGAAT-3'; P2, 5'-TATC-ATTCTGATCCCCATCTTCT-3'. *Med12^{Δ1-7}* was generated by Cre recombinase-mediated excision. ES cells with this allele were screened using the following primers in a multiplex PCR: P3, 5'-GTTT-CCGGCAGTAATCGAGAGTTTC; P4, 5'-TACATTCAAAGCCGT-CAGTTCATCC; and P2. Fully ES cell-derived embryos or mice were generated by tetraploid embryo complementation assays as previously described (Eakin and Hadjantonakis, 2006).

RNA and protein analysis

Protein extracts were prepared using a Nuclear/Cytosol Fractionation Kit (Biovision) and resolved in 4-12% SDS-PAGE gels (Invitrogen) and subsequently blotted on PVDF membranes (Millipore). The antibodies used were: anti-Med12 (Novus Biologicals, NB100-2357), anti-histone H3 (Abcam, 1791), anti-Nanog (Abcam, 21624), anti-Oct4 (Stemgent, 09-0023), anti-Rpb1 (Polr2a – Mouse Genome Informatics) (Cell Signaling, 2629), anti-β-catenin (BD Transduction Laboratories, 610153), anti-Tcf7 (Cell Signaling, 2206), anti-Axin2 (Abcam, 32197) and anti-α-tubulin (Sigma, 5168).

RNA was extracted using Trizol (Invitrogen) and used to produce cDNA with the SuperScript First-Strand Kit (Invitrogen). Primers for quantitative PCR are listed in Table S1 in the supplementary material. PCR reactions were performed using SYBR Green (Applied Biosystems) and data were analyzed with Step One Software v2.1 (Applied Biosystems) using the $\Delta\Delta C_T$ method.

Electron microscopy, histology and whole-mount in situ hybridization

Scanning electron microscopy and Hematoxylin and Eosin staining were performed according to standard protocols. Whole-mount in situ hybridization was performed using the protocol and probes of the MAMEP database (<http://mamep.molgen.mpg.de>). The *Uncx* probe has been described (Neidhardt et al., 1997) and the *Hesx1* probe was a kind gift from Michael Kessel (MPI for Biophysical Chemistry, Göttingen, Germany).

TUNEL and immunostainings

TUNEL assay was carried out according to the protocol of the In Situ Cell Death Detection Kit, AP (Roche). Immunostainings were performed as previously reported (Kispert and Herrmann, 1994). Antibodies against the following proteins were used: anti-Med12 (Novus Biologicals, NB100-2357), anti-phospho-histone H3 Ser10 (Millipore, 09797), anti-cleaved caspase 3 (Cell Signaling, 9661), anti-β-catenin (Santa Cruz, H-102), anti-E-cadherin (BD Transduction Laboratories, 610182), anti-Vangl2 (a gift from M. Montcouquiol, INSERM, Bordeaux, France) and anti-T (Kispert and Herrmann, 1994).

Reporter gene assays

Luciferase assays were performed in a 96-well plate format by plating 50,000 ES cells 24 hours prior to transfection. For the Gal4 reporter assays, cells were transfected with 150 ng Gal4-luciferase reporter and 40 ng Gal4-VP16 activator plasmid (Stratagene). Total amounts of transfected DNA were kept equal by adding pBluescript plasmid DNA. In the Wnt signaling assay, cells were transfected with 180 ng of an improved TOP-Flash reporter (gift of Jörg Hülsken, ISREC, Lausanne, Switzerland). After 4 hours, the transfection medium was changed to conditioned medium. Parental and Wnt3a-expressing L cells (ATCC #CRL-2648 and #CRL-2647, respectively) were used to prepare conditioned medium as described previously (Willert et al., 2003), and medium was used 1:1 diluted in ES cell medium. pRL-TK (10 ng) (Promega) was co-transfected as an internal control for normalization of transfection efficiency. Transfections were performed using Lipofectamine 2000 (Invitrogen) according to the

manufacturer's protocol. Twenty-four hours after transfection, cells were lysed and luciferase was measured using the Dual-Luciferase Assay System (Promega).

RESULTS

Generation of *Med12* mutant embryonic stem cells and mice

Med12 is ubiquitously expressed in early mouse embryos (see Fig. S1 in the supplementary material). To investigate the functions of *Med12* in vivo and its potential role during mammalian development, we targeted the X-linked *Med12* gene in male mouse ES cells following the strategy depicted in Fig. S2A in the supplementary material. This strategy was designed to provide ES cells carrying a conditional null allele. Two independent homologous recombinant ES cell clones were identified and their hemizyosity verified by Southern blotting using an external probe (see Fig. S2B in the supplementary material). Transient Flp recombinase expression removed the neomycin selection (neo) cassette and generated ES cells with the conditional null allele, *Med12^{fllox}* (Fig. 1A).

Med12^{fllox} ES cells were used to generate mutant mice, which had no obvious phenotype and were fertile. When crossing hemizygous *Med12^{fllox}* males with heterozygous *Med12^{fllox}* females, all genotypes were recovered at the expected Mendelian frequency (see Fig. S2C in the supplementary material), and homozygous *Med12^{fllox}* females were phenotypically indistinguishable from littermates. By contrast, we were not able to derive mice from the originally targeted hemizygous ES cell clones, which still contained the neo cassette, indicating that the targeted mutation results in embryonic lethality. To determine whether the targeted allele is hypomorphic, we analyzed *Med12* protein levels in these cells and found that the *Med12* protein is indeed reduced by more than 90% compared with wild-type and *Med12^{fllox}* cells (Fig. 1B); therefore, we refer to this allele as *Med12^{hyppo}*.

Northern blot analysis showed that *Med12* mRNA levels are decreased in *Med12^{hyppo}* ES cells. Interestingly, in addition to less *Med12*, these ES cells also produced a new *Med12* mRNA that was shorter than the wild-type message (see Fig. S3A in the supplementary material). Using 5' RACE, we mapped the transcriptional start site of this message to the PGK promoter of the neo cassette. No functional *Med12* can be produced because a premature stop codon is present in this message (see Fig. S3B in the supplementary material).

Med12^{hyppo} embryos have neural tube closure defects and die at E10.5 with cardiac malformations

To study the embryonic lethality resulting from reduced *Med12* levels, we used tetraploid embryo complementation assays to generate embryos from *Med12^{hyppo}* and *Med12^{fllox}* ES cells. *Med12^{fllox}* embryos had no obvious defects (Fig. 1E,G), as expected because *Med12* levels are normal in *Med12^{fllox}* embryos (Fig. 1B). By contrast, all *Med12^{hyppo}* embryos recovered at E9.5 were aberrant, although the morphological abnormalities exhibited variable penetrance (Fig. 1C,F,H; Fig. 2). No living embryo was found at E10.5. The phenotypic spectrum of embryos from the two independent *Med12^{hyppo}* clones was identical; therefore, we refer to both as *Med12^{hyppo}*.

Neural tube closure defects were the most striking phenotype observed, with complete penetrance in E9.5 embryos (Fig. 1C). Normally, neural tube closure completes at E9.5. Most *Med12^{hyppo}* mutants showed closure in only a small part of the body axis, at the

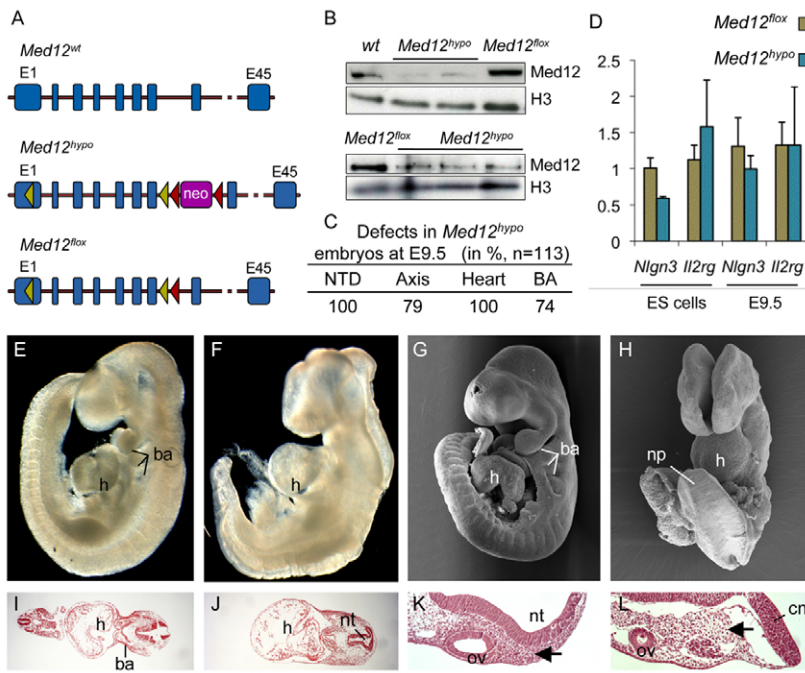


Fig. 1. Reduced Med12 levels in *Med12*^{hypo} embryos cause lethality at E9.5. (A) Schematic representation of the *Med12* alleles used. Blue boxes, exons; green triangles, *loxP* sites; red triangles, *frt* sites; neo, neomycin resistance cassette. (B) Targeted recombination reduces *Med12* expression in *Med12*^{hypo} ES cells and embryos. Nuclear protein lysates from different ES cell lines (top) and embryos (bottom) were analyzed by western blotting. (C) Summary of the defects observed in E9.5 *Med12*^{hypo} embryos. NTD, neural tube defects; Axis, axis truncation; Heart, enlarged and poorly differentiated heart; BA, first branchial arch absent. (D) mRNA levels of *Nlgn3* and *Il2rg* were measured by quantitative RT-PCR. RNA was isolated from ES cells and E9.5 embryos. *Gapdh* was used as an internal control. (E-L) Mouse embryos were generated from *Med12*^{lox} (E,F,I,J) and *Med12*^{hypo} (G,H,K,L) ES cells by tetraploid complementation. (E,F) Lateral view of E9.5 embryos after dissection. (G,H) Scanning electron micrographs of embryos at E9.5. (I-L) Hematoxylin and Eosin staining of transverse sections of the embryos in E and F at the level of the heart (I,J) and the forebrain region (K,L). Arrows show deficiencies in the head mesenchyme of *Med12*^{hypo} embryos. ba, branchial arches; cnf, cranial neural folds; h, heart; np, neural plate; nt, neural tube; ov, optic vesicle.

level of the heart (Fig. 1F,H,J), whereas a small proportion (18 out of 113) had no neural tube closure points. Elevation of the neural folds occurred in some areas, but a completely, flat neural plate was frequently observed (Fig. 1H). Additionally, where the neural tube achieved closure it failed to establish the correct straight tubular shape (e.g. Fig. 1J, Fig. 2A). The head mesenchyme located between the cranial neural folds and the surface ectoderm was reduced and sparse in *Med12*^{hypo} embryos in comparison with controls (Fig. 1K,L).

During the process of neural tube closure, neural crest cells start to migrate from the neural plate and participate in multiple developmental processes, including formation of the branchial arches. In *Med12*^{hypo} mutants, the first branchial arch was either extremely reduced or absent and the second and third branchial arches were never present (Fig. 1F,H). Expression analysis of the

neural crest cell marker *Crabp1* highlighted that in *Med12*-deficient mutants, these cells fail to migrate and are retained in the neural folds (see Fig. S4A in the supplementary material).

All mutant embryos had an enlarged heart that did not loop and mostly stayed in the midline (Fig. 1C,F,H,J), clearly indicating cardiac dysfunction. The perturbed development of the cardiovascular system is very likely responsible for the death of *Med12*^{hypo} embryos. Abnormal allantois formation, a recurrent cause for embryonic lethality at the midgestation stage, was never observed (Fig. 2E).

To check that the PGK promoter of the neo cassette was not influencing the transcription of neighboring genes, we measured mRNA levels of neuroligin 3 (*Nlgn3*) and interleukin 2 receptor gamma chain (*Il2rg*), the immediate 5' and 3' flanking genes of *Med12*. Expression of these genes was not significantly altered in

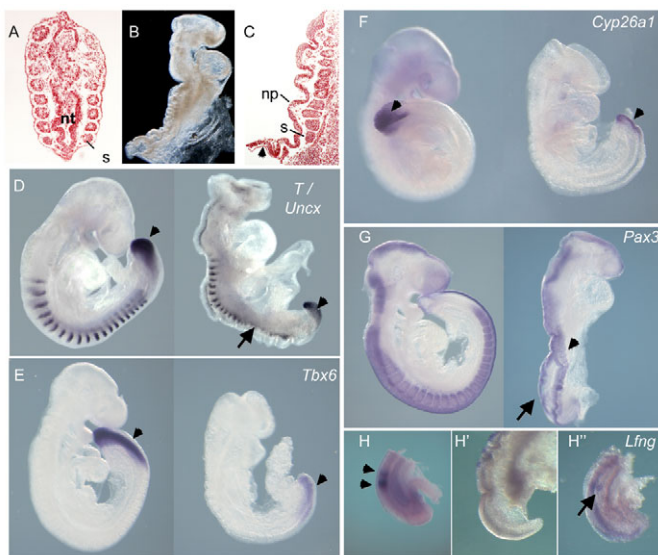


Fig. 2. Med12 is essential for somitogenesis and axis elongation. (A) Frontal section of a *Med12*^{hypo} E9.5 mouse embryo showing a strongly kinked neural tube. (B) *Med12*^{hypo} mutant with severe axis truncation, abnormal somitogenesis and an undulating neural plate. (C) Sagittal section of the embryo in B. Arrowhead shows the absence of mesenchyme at the caudal end. nt, neural tube; np, neural plate; s, somites. (D-G) Expression of developmental marker genes in *Med12*^{lox} (left) and *Med12*^{hypo} (right) embryos assessed by whole-mount in situ hybridization (WISH). (D) *T* and *Uncx* expression. In *Med12*^{hypo} embryos, somites are extremely small and disorganized and most caudal somites are not formed (arrow). The *T* expression domain at the caudal end is reduced in comparison to that of controls (arrowheads). *Tbx6* (E) and *Cyp26a1* (F) are strongly downregulated in the presomitic mesoderm of *Med12*^{hypo} mutants (arrowheads). (G) *Pax3* hybridization highlights the somitogenesis defects (arrowhead) and the undulating neural tube that is flat at the posterior end of *Med12*^{hypo} embryos (arrow). (H-H'') The oscillating expression of *Lfng* (arrowheads) seen in the control embryo (H) is absent in the majority of *Med12*^{hypo} embryos (H'). One of eight embryos displayed a faint expression domain (H'', arrow).

Med12^{hypo} ES cells and embryos (Fig. 1D). Moreover, mouse models that produce null alleles of these genes display no embryonic phenotype (DiSanto et al., 1995; Varoqueaux et al., 2006), confirming that the *Med12^{hypo}* phenotypes described here are indeed caused by the diminished levels of Med12.

Rather than being the result of a general defect in transcription, the phenotypes presented here implicate Med12 as essential for specific steps in mouse development and hence for gene-specific functions of the Mediator. In agreement with this, a tightly regulated developmental process such as brain patterning occurs undisturbed in *Med12^{hypo}* embryos (see Fig. S4 in the supplementary material). Moreover, no difference was seen among *Med12^{hypo}* and control embryos in the number and distribution of dividing cells, and in Med12-deficient embryos apoptotic cells were mostly present in the heart and not generally widespread (see Fig. S5 in the supplementary material). Removal of the neo cassette from *Med12^{hypo}* ES cells restored normal Med12 levels and allowed generation of the phenotypically normal *Med12^{fllox}* mouse line (Fig. 1B). Therefore, we can conclude that the defects observed in *Med12^{hypo}* embryos are caused by a lack of Med12 protein and not by somatic mutations of the targeted ES cells or abnormalities arising from the tetraploid complementation assay.

Reduced Med12 levels lead to somitogenesis defects and body axis truncation

The formation of somites, which are transient embryonic structures formed from unsegmented mesoderm, is an essential process during organization of the vertebrate body plan that occurs in a tightly regulated process controlled by several signaling pathways in an oscillating manner (Aulehla et al., 2003). Somitogenesis in *Med12^{hypo}* embryos was abnormal (Fig. 2) and whole-mount *in situ* hybridization (WISH) analysis for the expression of *Uncx*, a marker for the caudal half of somites, revealed that the decrease in Med12 leads to smaller, irregular and undifferentiated somites, with increased severity towards the caudal end of the embryos (Fig. 2A,C,D). *Lfng*, a gene with an oscillating expression pattern that is important for somitogenesis, was absent in *Med12^{hypo}* mutants and only one embryo ($n=8$) showed a faint expression domain (Fig. 2H), indicating that the transcriptional network controlling oscillating expression is disturbed. Somitogenesis irregularities frequently lead to a kinked neural tube, as occurred in *Med12^{hypo}* embryos (Fig. 2A) (Conlon et al., 1995).

Med12^{hypo} embryos displayed severe posterior axis truncation, showing that Med12 is necessary for axis elongation. Histological analysis of the caudal end of embryos with a strong truncated axis phenotype revealed a complete absence of the tissue responsible for axis elongation, namely the caudal end mesenchyme (Wilson et al., 2009) (Fig. 2B,C). In these embryos, somitogenesis irregularities were also more evident, and the neural plate tissue was overgrown in comparison to the underlying segmented paraxial mesenchyme and had an undulating shape (Fig. 2B,C). brachyury (*T*) expression levels in *Med12^{hypo}* embryos were similar to those of controls, but the expression domain was reduced, which is indicative of a defect in mesoderm formation (Fig. 2D). *Tbx6*, a downstream target of *T* that is expressed in the presomitic mesoderm, also had a reduced expression domain and was downregulated in *Med12^{hypo}* embryos (Fig. 2E). Moreover, expression of *Cyp26a1*, another important regulator of axis elongation expressed in the presomitic mesoderm, was also diminished (Fig. 2F). These results indicate that axis truncation in *Med12^{hypo}* mutants is caused by compromised presomitic mesoderm formation.

Pax3, besides being expressed in the somites, is also a marker for the dorsal half of the neural tube, which allowed us to investigate the relationship between somitogenesis defects and the abnormal formation of the neural plate. The presence of two dorsolateral domains, instead of a single dorsal midline domain, showed that in some parts of the trunk the neural plate was not able to elevate and had an undulating shape (Fig. 2G). Moreover, expression of *Pax3* confirmed that the ratio between neural tissue and paraxial mesenchyme is disturbed in *Med12^{hypo}* embryos. In conclusion, the axis truncation defects of *Med12^{hypo}* embryos are caused by a defect in the formation of presomitic mesoderm, and the excess of neural ectoderm might lead to the undulation of the neural plate, precluding its closure.

The Wnt/PCP pathway is disturbed in *Med12^{hypo}* embryos

Around 15% of the *Med12^{hypo}* embryos failed to close the neural tube along the whole body axis (for examples, see Fig. S6 in supplementary material), which leads to the defect known as craniorachischisis (CRS). Interestingly, out of over 150 genes known to cause neural tube defects, all those implicated in CRS are components of the PCP signaling pathway (Harris and Juriloff, 2007), suggesting that Med12 could be involved in PCP regulation. This well-conserved, non-canonical Wnt-frizzled-dishevelled pathway is responsible for the establishment of cell polarity within an epithelial plane, and in vertebrates it has been implicated in the regulation of processes including convergent extension (CE), neural tube closure, eyelid closure and hair bundle orientation in inner ear sensory cells (Wang and Nathans, 2007). Specifically, CE movements in the neuroectoderm lead to narrowing and elongation of the floorplate, enabling neural fold apposition and neural tube closure (Ybot-Gonzalez et al., 2007). To assess the role of Med12 in PCP we tested whether key components of the core PCP signaling pathway were correctly expressed in *Med12^{hypo}* embryos. *Fzd3* and *Vangl2*, two PCP genes implicated in neural tube closure, were expressed in the neural folds of both *Med12^{hypo}* and control embryos (Fig. 3A,B). CE through cell intercalation at the midline leads to elongation of the anterior-posterior axis and is controlled by PCP signaling. *Wnt5a* is an *Fzd3* ligand implicated in PCP signaling and is necessary for full axis elongation (Yamaguchi et al., 1999a). Its expression, although still present, appeared compromised at the caudal end of the embryo (Fig. 3C), in a similar fashion to the other regulators of axis elongation that we describe in Fig. 2. One hallmark of a defective CE is a laterally extended midline. Although embryos with a full open neural tube presented a U-shaped floorplate, the expression domain of *T* and *Shh* in the notochord was not expanded in *Med12^{hypo}* embryos (Fig. 3D,E).

The asymmetric distribution of core PCP components such as Prickle1 in the neural plate has recently been shown to be regulated by a Wnt5a-mediated pathway and to be essential for neural tube closure (Narimatsu et al., 2009). In the absence of Smad ubiquitylation regulatory factors (Smurf), this pathway was disturbed, and the localization of Prickle1 in cells of the neural tube changed from a membrane to a diffuse cellular pattern, with increased staining intensity (Narimatsu et al., 2009). Control embryos displayed the expected membrane localization of Prickle1; however, in *Med12^{hypo}* embryos, Prickle1 became distributed throughout the cytoplasm (Fig. 3G), as seen in Smurf mutants. *Vangl2* localization, by contrast, was unaffected (Fig. 3F). These results show that Wnt/PCP signaling is disturbed by the low levels of Med12 and suggest that the severe neural tube closure defects are likely to be caused by this disturbance.

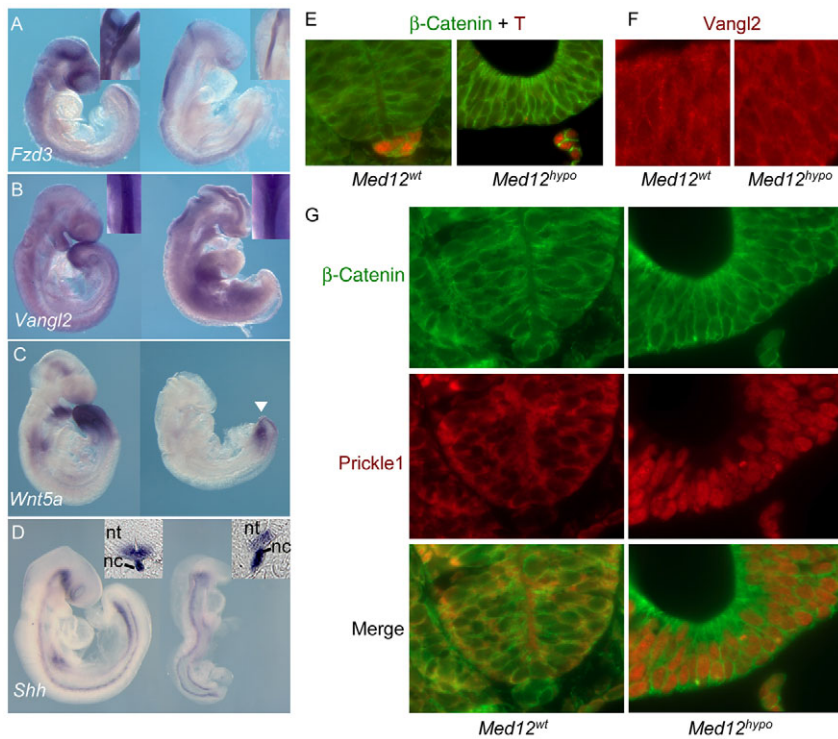


Fig. 3. Disturbed Wnt/PCP signaling in *Med12^{hyp}* embryos. (A-D) WISH of components of the Wnt/PCP pathway showing *Med12^{hyp}* (right) and control (left) mouse embryos. (A,B) Expression of PCP components *Fzd3* and *Vangl2* is undisturbed in *Med12^{hyp}* embryos, with a strong signal in the neural folds (insets). (C) *Wnt5a* is downregulated at the caudal end of mutant embryos (arrowhead). (D) *Shh* expression is not impaired upon reduction of *Med12* levels. Vibratome sections at the level of the hindlimbs of control and *Med12^{hyp}* embryos show normal expression in the floor plate of the neural tube (nt) and in the notochord (nc) (insets). (E-G) Immunostaining using antibodies against the indicated proteins. (E) T expression in the notochord of *Med12^{hyp}* embryos is not laterally expanded. (F) *Vangl2* is localized in the membrane of both *Med12* mutant and control embryos. (G) *Prickle1* loses its membrane localization and becomes spread throughout the cytoplasm in the neural plate of *Med12^{hyp}* embryos.

Med12 is necessary for canonical Wnt/ β -catenin signaling in the developing embryo

Human β -catenin, the effector of canonical Wnt signaling, has been shown to bind the Mediator complex via interaction with Med12 (Kim et al., 2006). β -catenin recruits the Mediator to promoters of its target genes, and in luciferase reporter assays Med12 was shown to be required for the correct response to Wnt signals. Since some of the defects in *Med12^{hyp}* embryos phenocopy deficiencies of ligands and effectors of the Wnt signaling pathway, we investigated whether the β -catenin requirement for Med12 could have functional relevance in the developing mouse embryo.

We analyzed the expression of direct target genes of Wnt/ β -catenin signaling. For cyclin D1 (*Ccnd1*) and *Axin2* there was an accentuated reduction of expression in the mesenchyme, whereas neural tissues appeared to be unaffected. The posterior end of the embryo is a striking example of this, where no expression of either gene was detected, except in the neural plate (Fig. 4A,B). This is in agreement with what we describe in Fig. 2 and could be an explanation for the reduced mesenchymal tissue in comparison to neuroectoderm. *Myc* expression, by contrast, was generally affected throughout the whole embryo, indicative of defective Wnt signaling (Fig. 4C). *Dkk1* is an inhibitor of Wnt signaling and is directly

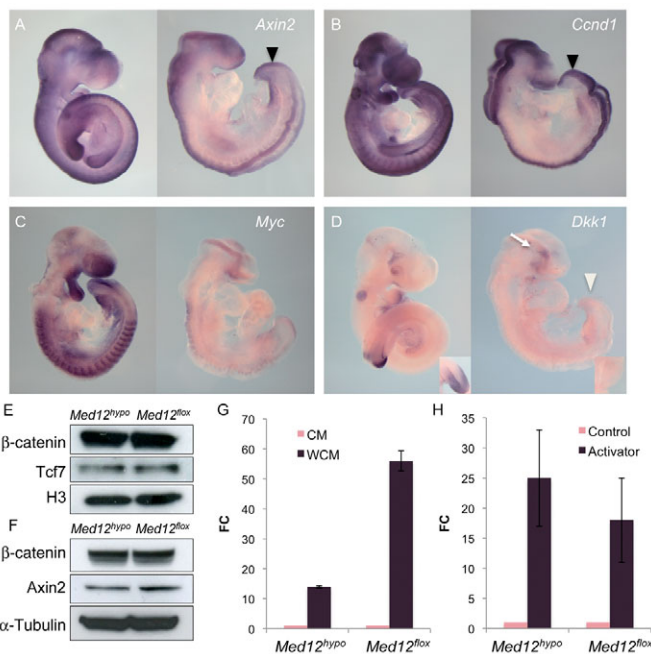


Fig. 4. Med12 is essential for the activation of Wnt targets. (A-D) WISH of canonical Wnt target genes in control (left) and *Med12^{hyp}* (right) mouse embryos. Black arrowheads in A and B indicate expression of *Axin2* and *Ccnd1* solely in the neural plate at the posterior end of *Med12^{hyp}* embryos. White arrowhead in D points to the caudal end, where *Dkk1* expression in *Med12^{hyp}* embryos is absent. Arrow in D indicates expression of *Dkk1* in the head of *Med12^{hyp}* embryos. (E,F) Nuclear (E) and cytosolic (F) protein lysates of E9.5 embryos analyzed by western blotting. (G) *Med12^{hyp}* ES cells have a compromised response to canonical Wnt signaling. Fold change (FC) was calculated using the luciferase activity of cells treated with conditioned medium (CM) from parental L cells as a reference. WCM, Wnt3a-conditioned medium. (H) Med12 is not essential for VP16-mediated transactivation. ES cells were transfected with a Gal4-luciferase reporter and subsequently transfected with a Gal4-VP16 expression plasmid.

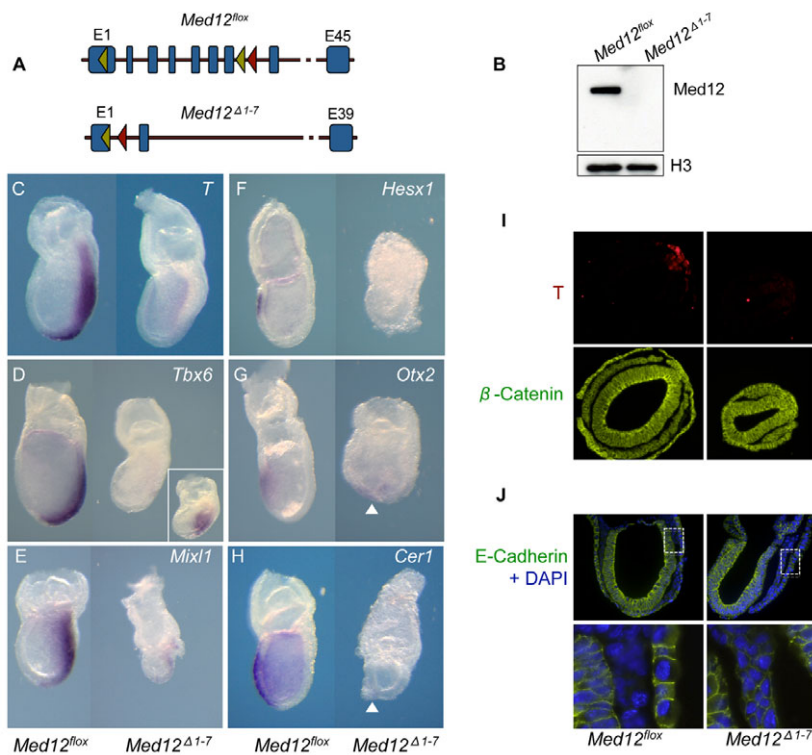


Fig. 5. *Med12^{Δ1-7}* embryos die at early gastrulation and fail to establish an anterior-posterior axis. (A) Schematic representation of the alleles used. Blue boxes, exons; green triangles, loxP sites; red triangles, *frt* sites. (B) No Med12 is detected in *Med12^{Δ1-7}* mouse ES cells. Nuclear protein lysates from ES cell lines were analyzed by western blotting. (C-H) WISH of genes in *Med12^{flox}* (left) and *Med12^{Δ1-7}* (right) embryos involved in establishment of the anterior-posterior axis at E7.5. The primitive streak marker genes *T* (C), *Tbx6* (D) and *Mixl1* (E) are either not expressed or severely downregulated in the absence of Med12. Inset in D shows one *Med12^{Δ1-7}* embryo capable of *Tbx6* expression. *Hesx1*, a marker for the anterior visceral endoderm (AVE), is absent in *Med12^{Δ1-7}* embryos (F). *Otx2* and *Cer1* are expressed at the distal-most tip of *Med12^{Δ1-7}* embryos (arrowheads) and not anteriorly, as occurs in the controls. (I) Double immunostaining with anti-T and anti-β-catenin antibodies shows that in the absence of Med12 (right), although T is not expressed, mesoderm seems to be formed. (J) Anti-E-cadherin antibody staining highlights the inability to downregulate this protein in the mesodermal tissue of *Med12^{Δ1-7}* embryos.

regulated by canonical Wnt signaling in a negative-feedback loop mechanism. *Dkk1* expression in the tail mesenchyme, where Wnt signaling is highly active, was lost in *Med12^{hypo}* mutants (Fig. 4D). More than ten embryos were analyzed for each gene to avoid false interpretations caused by the dynamic expression of *Axin2* and *Dkk1*.

Having seen that expression of Wnt/β-catenin target genes was affected, we investigated whether components of this pathway are intact in *Med12^{hypo}* ES cells that are in a basal transcriptional state. *Med12^{hypo}* and *Med12^{flox}* ES cells exhibited no differences in the levels of Tcf7, *Axin2* and nuclear or cytosolic β-catenin (Fig. 4E,F). However, as previously described for other cell lines (Kim et al., 2006), Med12 is also essential for the activation of a Wnt reporter in mouse ES cells. We derived this conclusion after *Med12^{flox}* and *Med12^{hypo}* ES cells were transfected with a luciferase reporter containing a β-catenin-responsive promoter (TOP-Flash) and treated with Wnt3a-conditioned medium (WCM). We verified that although *Med12^{hypo}* cells are able to respond to WCM, they do so in a very compromised fashion in comparison to the *Med12^{flox}* ES cells in which Med12 expression was rescued by excision of the neo cassette (Fig. 4G). To test whether this impairment of transcriptional activation is specific for Wnt signaling, we measured luciferase expression from a Gal4 reporter upon activation with a Gal4-VP16 activator. *Med12^{hypo}* cells were as capable of activating the Gal4 luciferase reporter as their *Med12^{flox}* counterparts (Fig. 4H). Similar results were obtained upon measuring the ability of serum response factor (Srf) to activate an Srf reporter (data not shown). Taken together, these results show that activated transcription is not generally impaired in *Med12^{hypo}* mutants and that signaling via the Wnt/β-catenin pathway is abnormal.

Absence of Med12 causes embryonic arrest at E7.5 and loss of canonical Wnt/β-catenin signaling

Our data suggest that Wnt signaling is not totally abrogated in *Med12^{hypo}* embryos as some of the investigated Wnt targets are still expressed in the neuroectoderm, and *T*, an established

canonical Wnt target (Yamaguchi et al., 1999b), is expressed at the caudal end without apparent reduction. Two hypotheses can help to explain these results. First, it could be due to a potential basal level of Wnt induction that is independent of Med12 and might vary in different embryonic tissues. Second, the residual Med12 in *Med12^{hypo}* embryos might be sufficient for the remaining Wnt activity.

To test the latter, we generated *Med12*-null ES cells by transient expression of Cre recombinase in *Med12^{flox}* ES cells. This promoted recombination between the two loxP sites leading to excision of exons 2-7 and a part of exon 1, thus generating the *Med12^{Δ1-7}* allele (Fig. 5A; see Fig. S7A,B in the supplementary material). In these ES cells, we could not detect any Med12 by western blotting (Fig. 5B). We then used tetraploid complementation with *Med12^{Δ1-7}* and *Med12^{flox}* ES cells to generate *Med12*-null embryos and controls. Interestingly, the absence of Med12 led to a more severe phenotype than that observed in *Med12^{hypo}* mutants. No *Med12^{Δ1-7}* embryos were found at the head-fold stage, and at E7.5 many embryos were arrested at pre-streak stages. Strikingly, *T* expression was severely reduced in Med12-deficient embryos (Fig. 5C), suggesting that these embryos cannot induce mesoderm formation and that Wnt/β-catenin signaling is abrogated. Other primitive streak markers were also affected. *Tbx6* was also absent in *Med12^{Δ1-7}* embryos (Fig. 5D), although one embryo with a strong constriction in the embryonic cup was capable of expressing *Tbx6*. *Mixl1* expression was severely reduced, although it could be detected at the posterior side of the *Med12^{Δ1-7}* embryos (Fig. 5E).

In the absence of β-catenin, mouse embryos not only fail to form a primitive streak, but also do not initiate migration of the distal visceral endoderm (DVE) to form the anterior visceral endoderm (AVE), thus failing to establish an anterior-posterior axis (Huelsen et al., 2000). In *Med12^{flox}* embryos, the AVE was marked by strong expression of *Hesx1*, which was totally absent in the *Med12^{Δ1-7}* mutants (Fig. 5F). *Otx2* and *Cer1*, two genes known to be expressed on the anterior side of the E7.5 embryo,

were strongly downregulated and found only at the most distal tip of the embryo, indicating failure of DVE migration (Fig. 5G,H).

Analysis of transverse sections of *Med12^{Δ1-7}* embryos by immunostaining confirmed that T is not expressed in the absence of Med12 (Fig. 5I). Surprisingly, although T is not present, staining with an anti-β-catenin antibody allowed visualization of the primitive streak and a third germ layer, suggesting that mesoderm is formed (Fig. 5I). However, this tissue was incapable of downregulating E-cadherin (cadherin 1 – Mouse Genome Informatics), indicating that it remains epithelial and therefore lacks the most defining characteristic of mesenchymal cells (Fig. 5J). These results allow us to conclude that in the mouse embryo, in the absence of Med12, genes controlled by Wnt signaling cannot be activated and therefore formation of the mesoderm is severely impaired.

Med12 is not required for Nanog expression or ES cell pluripotency

ES cell pluripotency is controlled by a complex transcriptional network, which includes stem cell-specific factors such as Nanog, Oct4 (Pou5f1 – Mouse Genome Informatics) and Sox2. The homeodomain protein Nanog is a master regulator of the pluripotency state and was recently shown to bind Med12 (Tutter et al., 2008). According to this report, upon siRNA-mediated Med12 knockdown in mouse ES cells, *Nanog* expression was downregulated and cells started a differentiation program, as assessed by the expression of pluripotency and differentiation markers. To verify whether these results are reproducible in our *Med12*-targeted model, we assessed the pluripotency of *Med12^{hyppo}* ES cells, as these cells have similar levels of Med12 to those described by Tutter and colleagues. In contrast to what was reported from siRNA knockdown, and despite the dramatic Med12 loss, Nanog levels in *Med12^{hyppo}* ES cells were comparable to those of *Med12^{fllox}* and control cells (Fig. 6A). We then examined by quantitative RT-PCR the expression of genes that were described by Tutter et al. as being dysregulated upon *Med12* knockdown (Tutter et al., 2008). None of the ES cell pluripotency markers, including *Oct4*, *Sox2*, *Rest* and *Rex1* (*Zfp42* – Mouse Genome Informatics), showed decreased expression in *Med12^{hyppo}* ES cells, as compared with their *Med12^{fllox}* counterparts (Fig. 6B). Markers for ES cells going through a differentiation program, such as *T* and *Eomes*, were not upregulated, showing that the *Med12^{hyppo}* ES cells do not start such a program. Finally, we were able to confirm *Bmp4*, *Fgf5* and *Nefl* as Med12 targets as these genes were dysregulated and behaved as previously described (Tutter et al., 2008) (Fig. 6B).

Moreover, testifying for the pluripotency of *Med12^{hyppo}* ES cells, Oct4 levels were unaltered (Fig. 6A), the proliferative state was unaffected (Fig. 6C) and, as we describe here, these ES cells could contribute to all embryonic lineages. In addition, *Med12^{fllox}* ES cells, which are derived from *Med12^{hyppo}* ES cells, are able to generate fully ES cell-derived living mice, demonstrating that the prior low Med12 levels did not compromise the stemness state. Furthermore, in *Med12^{Δ1-7}* ES cells, in which no Med12 can be detected, we found no difference in the expression of Nanog as compared with *Med12^{fllox}* controls (Fig. 6A).

We conclude that, in our model, Nanog expression is not dependent on Med12 and that reduced Med12 levels do not lead to the dysregulation of Nanog target genes, nor to the loss of pluripotency.

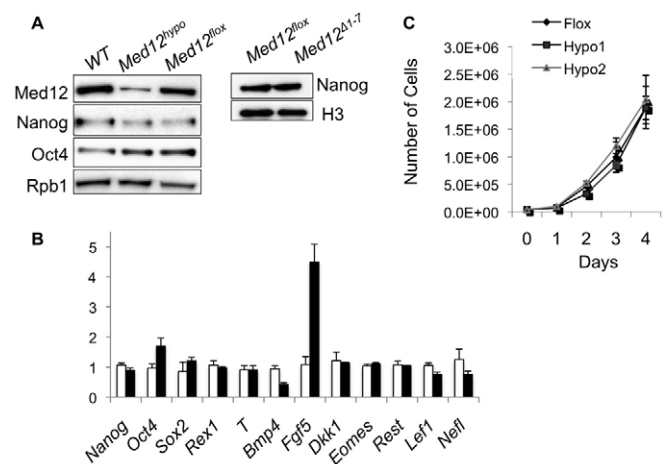


Fig. 6. *Med12* mutant ES cells have unaltered expression of *Nanog* and *Nanog* target genes. (A) Expression of pluripotency markers was tested in *Med12^{hyppo}* and *Med12^{Δ1-7}* mouse ES cells by western blot. (B) The expression of pluripotency and differentiation markers was analyzed by quantitative RT-PCR in *Med12^{fllox}* (white) and *Med12^{hyppo}* (black) ES cells. *Gapdh* was used as an internal control and fold change was calculated using one of the *Med12^{fllox}* samples as reference. (C) *Med12^{hyppo}* ES cells proliferate normally. One *Med12^{fllox}* and two *Med12^{hyppo}* ES cell clones were grown for 4 days and their cell number counted daily. Error bars indicate the mean \pm s.d. of three independent experiments.

DISCUSSION

We describe for the first time the role of Med12 during early mouse development. Using a gene-targeting approach we generated ES cells that have highly compromised Med12 expression and cells that are completely depleted of this Mediator subunit. The developmental defects identified in embryos generated from these two cell lines allowed us to identify Med12 as a subunit involved in gene-specific functions and to show that Med12 is necessary for the establishment of both canonical Wnt and Wnt/PCP signaling.

β-catenin has been shown to interact with Med12 (Kim et al., 2006). We confirmed that Med12 is required for activation of Wnt/β-catenin targets both on artificial promoters and in the developing embryo. The absence of Med12 recapitulates phenotypes of β-catenin-null embryos (Huelsen et al., 2000), which also fail to express marker genes of the AVE and of the primitive streak, including *T*, a direct Wnt/β-catenin target that is absent in *Med12^{Δ1-7}* embryos. At midgestation, we observed that in *Med12^{hyppo}* embryos the expression of other targets of canonical Wnt signaling is severely compromised and, concomitantly, that Wnt-regulated processes, such as the oscillating expression of somitogenesis genes (Aulehla et al., 2003) and axis elongation via proliferation of the caudal end mesenchyme, are severely affected (Wilson et al., 2009). The fact that *Med12^{Δ1-7}* embryos cannot complete gastrulation and fail to activate *T* expression suggests that the residual Med12 in the hypomorphic mutants is sufficient for the first processes regulated by Wnt signaling to be successfully completed, and only at later stages do Wnt-related deficiencies become apparent. It is also important to mention that Wnt-dependent activation of the TOP-Flash reporter is slightly reduced in *Med12^{Δ1-7}* ES cells as compared with the hypomorphic mutants, but is still detectable (see Fig. S7C in the supplementary material), suggesting that a Med12-independent basal level of Wnt activation

exists. This could provide an explanation for why, in the absence of Med12, in contrast to Wnt3-null or β -catenin-null embryos (Huelsken et al., 2000), epiblast cells are still able to ingress through the primitive streak but later fail to become mesenchymal. We believe that these cells are exposed to insufficient Wnt signals and therefore cannot adopt a mesodermal fate, similar to the observation described for *T* and *Wnt3a* mouse mutants (Yamaguchi et al., 1999b).

CRS and the loss of asymmetric Prickle1 distribution in cells of the neural plate of *Med12^{hypo}* embryos link, for the first time, Med12 with the establishment of the Wnt/PCP signaling pathway. PCP in vertebrates is regulated by non-canonical Wnt signaling, and a set of core PCP pathway components, which includes Vangl2, frizzled 3/6 and dishevelled 1/2, plays important roles in neural tube closure. A recent report by Narimatsu et al. describes a mechanism whereby the Wnt/PCP pathway via Wnt5a and, consequently, neural tube closure, depend on the asymmetric ubiquitin-mediated localization of Prickle1 (Narimatsu et al., 2009). How Med12 could be influencing this mechanism is still unknown, but a potential role in directly mediating transcription of the Smurf ubiquitin ligases or of other PCP components, such as Par6 (Pard6a – Mouse Genome Informatics) and dishevelled 2, that are also necessary for asymmetric Prickle1 localization should not be neglected. It is also possible that Med12 has a more general function within PCP by serving as a co-activator for transcription factors acting downstream of this signaling pathway. Downstream effectors of PCP have so far not been extensively studied during mouse neural tube closure, but in *Xenopus* Wnt/PCP signaling is known to activate c-Jun during gastrulation (Habas et al., 2003). Although Jnk signaling does not appear to be necessary for mouse neural tube closure, a co-regulator role for a PCP downstream transcription factor could be another function for Med12 (Ybot-Gonzalez et al., 2007).

Our results question a role for Med12 as a subunit required for all Mediator functions (e.g. basal and activated transcription). Such a role has been suggested for Med12 (Knuesel et al., 2009), but *Med12^{Δ1-7}* embryos develop further than mouse models of other Mediator subunits (Tudor et al., 1999) and no morphological defects can be detected until the pre-streak stage. Moreover, in *Med12^{hypo}* embryos, many embryonic structures, processes and developmental marker genes are undisturbed, testifying for gene-specific functions for Med12. Contrary to what has been described previously (Tutter et al., 2008), we show that expression of Nanog is not dependent on Med12. In addition, *Med12^{hypo}* ES cells, which have very reduced levels of Med12, do not lose expression of other pluripotency markers, do not enter a clear differentiation program and are still pluripotent.

Recent studies identified two missense mutations in the human *MED12* gene that were associated with two X-linked mental retardation syndromes. The Opitz-Kaveggia and Lujan syndromes have overlapping (mental retardation, macrocephaly) and also specific (imperforate anus in Opitz-Kaveggia, craniofacial abnormalities in Lujan) manifestations (Opitz and Kaveggia, 1974; Risheg et al., 2007; Schwartz et al., 2007). These symptoms also implicate Med12 as a subunit with gene-specific functions within the Mediator.

In conclusion, we have shown that the canonical and Wnt/PCP signaling pathways depend on Med12 for appropriate function during early mouse embryogenesis. However, the variety of defects in *Med12^{hypo}* embryos suggests that other roles for Med12 remain to be characterized. The conditional *Med12^{fl/ox}* mouse line reported here will help to clarify functions of Med12 at later stages of

development, in specific cells or tissues upon crosses with tissue-specific Cre lines. This will allow identification of new Med12 interactors and clarify the role of Med12 in the Wnt/PCP signaling pathway. Finally, inducible Cre systems will help us to elucidate possible roles of Med12 not only in embryonic development, but also in the homeostasis of the adult mouse and in understanding the above-mentioned human syndromes.

Acknowledgements

We thank Karol Macura for the tetraploid embryo complementation assays; Barbara Kosiol and Gabriele Drescher for technical assistance; Chris Bunce, Bernhard Herrmann, Michaela Mayer, Joana Vidigal and Lars Wittler for discussions concerning the manuscript; and Bernhard Herrmann, Michael Kessel and Mireille Montcouquiol for reagents. This work was supported by a grant of the European Union (Marie Curie RTN NucSys).

Competing interests statement

The authors declare no competing financial interests.

Supplementary material

Supplementary material for this article is available at <http://dev.biologists.org/lookup/suppl/doi:10.1242/dev.053660/-DC1>

References

- Akoulitchev, S., Chuiikov, S. and Reinberg, D. (2000). TFIID is negatively regulated by cdk8-containing mediator complexes. *Nature* **407**, 102-106.
- Aulehla, A., Wehrle, C., Brand-Saberi, B., Kemler, R., Gossler, A., Kanzler, B. and Herrmann, B. G. (2003). Wnt3a plays a major role in the segmentation clock controlling somitogenesis. *Dev. Cell* **4**, 395-406.
- Bourbon, H. M. (2008). Comparative genomics supports a deep evolutionary origin for the large, four-module transcriptional mediator complex. *Nucleic Acids Res.* **36**, 3993-4008.
- Bourbon, H. M., Aguilera, A., Ansari, A. Z., Asturias, F. J., Berk, A. J., Bjorklund, S., Blackwell, T. K., Borggreve, T., Carey, M., Carlson, M. et al. (2004). A unified nomenclature for protein subunits of mediator complexes linking transcriptional regulators to RNA polymerase II. *Mol. Cell* **14**, 553-557.
- Conaway, R. C., Sato, S., Tomomori-Sato, C., Yao, T. and Conaway, J. W. (2005). The mammalian Mediator complex and its role in transcriptional regulation. *Trends Biochem. Sci.* **30**, 250-255.
- Conlon, R. A., Reaume, A. G. and Rossant, J. (1995). Notch1 is required for the coordinate segmentation of somites. *Development* **121**, 1533-1545.
- Ding, N., Zhou, H., Esteve, P. O., Chin, H. G., Kim, S., Xu, X., Joseph, S. M., Friez, M. J., Schwartz, C. E., Pradhan, S. et al. (2008). Mediator links epigenetic silencing of neuronal gene expression with x-linked mental retardation. *Mol. Cell* **31**, 347-359.
- DiSanto, J. P., Muller, W., Guy-Grand, D., Fischer, A. and Rajewsky, K. (1995). Lymphoid development in mice with a targeted deletion of the interleukin 2 receptor gamma chain. *Proc. Natl. Acad. Sci. USA* **92**, 377-381.
- Donner, A. J., Szostek, S., Hoover, J. M. and Espinosa, J. M. (2007). CDK8 is a stimulus-specific positive coregulator of p53 target genes. *Mol. Cell* **27**, 121-133.
- Eakin, G. S. and Hadjantonakis, A. K. (2006). Production of chimeras by aggregation of embryonic stem cells with diploid or tetraploid mouse embryos. *Nat. Protoc.* **1**, 1145-1153.
- Emlund, H., Baraznenok, V., Lindahl, M., Samuelson, C. O., Koeck, P. J., Holmberg, S., Hebert, H. and Gustafsson, C. M. (2006). The cyclin-dependent kinase 8 module sterically blocks Mediator interactions with RNA polymerase II. *Proc. Natl. Acad. Sci. USA* **103**, 15788-15793.
- George, S. H., Gertsenstein, M., Vintersten, K., Korets-Smith, E., Murphy, J., Stevens, M. E., Haigh, J. J. and Nagy, A. (2007). Developmental and adult phenotyping directly from mutant embryonic stem cells. *Proc. Natl. Acad. Sci. USA* **104**, 4455-4460.
- Habas, R., Dawid, I. B. and He, X. (2003). Coactivation of Rac and Rho by Wnt/PCP signaling is required for vertebrate gastrulation. *Genes Dev.* **17**, 295-309.
- Harris, M. J. and Juriloff, D. M. (2007). Mouse mutants with neural tube closure defects and their role in understanding human neural tube defects. *Birth Defects Res. Part A Clin. Mol. Teratol.* **79**, 187-210.
- Hong, S. K., Haldin, C. E., Lawson, N. D., Weinstein, B. M., Dawid, I. B. and Hukriede, N. A. (2005). The zebrafish *kohtalo/trap230* gene is required for the development of the brain, neural crest, and pronephric kidney. *Proc. Natl. Acad. Sci. USA* **102**, 18473-18478.
- Huelsenken, J., Vogel, R., Brinkmann, V., Erdmann, B., Birchmeier, C. and Birchmeier, W. (2000). Requirement for beta-catenin in anterior-posterior axis formation in mice. *J. Cell Biol.* **148**, 567-578.
- Ito, M., Yuan, C. X., Okano, H. J., Darnell, R. B. and Roeder, R. G. (2000). Involvement of the TRAP220 component of the TRAP/SMCC coactivator

- complex in embryonic development and thyroid hormone action. *Mol. Cell* **5**, 683-693.
- Kim, S., Xu, X., Hecht, A. and Boyer, T. G.** (2006). Mediator is a transducer of Wnt/beta-catenin signaling. *J. Biol. Chem.* **281**, 14066-14075.
- Kispert, A. and Herrmann, B. G.** (1994). Immunohistochemical analysis of the Brachyury protein in wild-type and mutant mouse embryos. *Dev. Biol.* **161**, 179-193.
- Knuesel, M. T., Meyer, K. D., Donner, A. J., Espinosa, J. M. and Taatjes, D. J.** (2009). The human CDK8 subcomplex is a histone kinase that requires Med12 for activity and can function independently of mediator. *Mol. Cell. Biol.* **29**, 650-661.
- Malik, S. and Roeder, R. G.** (2005). Dynamic regulation of pol II transcription by the mammalian Mediator complex. *Trends Biochem. Sci.* **30**, 256-263.
- Narimatsu, M., Bose, R., Pye, M., Zhang, L., Miller, B., Ching, P., Sakuma, R., Luga, V., Roncari, L., Attisano, L. et al.** (2009). Regulation of planar cell polarity by Smurf ubiquitin ligases. *Cell* **137**, 295-307.
- Neidhardt, L. M., Kispert, A. and Herrmann, B. G.** (1997). A mouse gene of the paired-related homeobox class expressed in the caudal somite compartment and in the developing vertebral column, kidney and nervous system. *Dev. Genes Evol.* **207**, 10.
- Opitz, J. M. and Kaveggia, E. G.** (1974). Studies of malformation syndromes of man 33, the FG syndrome. An X-linked recessive syndrome of multiple congenital anomalies and mental retardation. *Z. Kinderheilkd.* **117**, 1-18.
- Rau, M. J., Fischer, S. and Neumann, C. J.** (2006). Zebrafish Trap230/Med12 is required as a coactivator for Sox9-dependent neural crest, cartilage and ear development. *Dev. Biol.* **296**, 83-93.
- Risheg, H., Graham, J. M., Jr, Clark, R. D., Rogers, R. C., Opitz, J. M., Moeschler, J. B., Peiffer, A. P., May, M., Joseph, S. M., Jones, J. R. et al.** (2007). A recurrent mutation in MED12 leading to R961W causes Opitz-Kaveggia syndrome. *Nat. Genet.* **39**, 451-453.
- Schwartz, C. E., Tarpey, P. S., Lubs, H. A., Verloes, A., May, M. M., Risheg, H., Friez, M. J., Futreal, P. A., Edkins, S., Teague, J. et al.** (2007). The original Lujan syndrome family has a novel missense mutation (p.N1007S) in the MED12 gene. *J. Med. Genet.* **44**, 472-477.
- Shin, C. H., Chung, W. S., Hong, S. K., Ober, E. A., Verkade, H., Field, H. A., Huisken, J. and Stainier, D. Y.** (2008). Multiple roles for Med12 in vertebrate endoderm development. *Dev. Biol.* **317**, 467-479.
- Taatjes, D. J., Marr, M. T. and Tjian, R.** (2004). Regulatory diversity among metazoan co-activator complexes. *Nat. Rev. Mol. Cell Biol.* **5**, 403-410.
- Takagi, Y. and Kornberg, R. D.** (2006). Mediator as a general transcription factor. *J. Biol. Chem.* **281**, 80-89.
- Tudor, M., Murray, P. J., Onufryk, C., Jaenisch, R. and Young, R. A.** (1999). Ubiquitous expression and embryonic requirement for RNA polymerase II coactivator subunit Srb7 in mice. *Genes Dev.* **13**, 2365-2368.
- Tutter, A. V., Kowalski, M. P., Baltus, G. A., Iourgenko, V., Labow, M., Li, E. and Kadam, S.** (2008). A role for med12 in regulation of nanog and nanog target genes. *J. Biol. Chem.* **284**, 3709-3718.
- Varoqueaux, F., Aramuni, G., Rawson, R. L., Mohrmann, R., Missler, M., Gottmann, K., Zhang, W., Sudhof, T. C. and Brose, N.** (2006). Neuroligins determine synapse maturation and function. *Neuron* **51**, 741-54.
- Wang, Y. and Nathans, J.** (2007). Tissue/planar cell polarity in vertebrates: new insights and new questions. *Development* **134**, 647-658.
- Wang, X., Yang, N., Uno, E., Roeder, R. G. and Guo, S.** (2006). A subunit of the mediator complex regulates vertebrate neuronal development. *Proc. Natl. Acad. Sci. USA* **103**, 17284-17289.
- Westerling, T., Kuuluvainen, E. and Makela, T. P.** (2007). Cdk8 is essential for preimplantation mouse development. *Mol. Cell. Biol.* **27**, 6177-6182.
- Willert, K., Brown, J. D., Danenberg, E., Duncan, A. W., Weissman, I. L., Reya, T., Yates, J. R., 3rd and Nusse, R.** (2003). Wnt proteins are lipid-modified and can act as stem cell growth factors. *Nature* **423**, 448-452.
- Wilson, V., Olivera-Martinez, I. and Storey, K. G.** (2009). Stem cells, signals and vertebrate body axis extension. *Development* **136**, 1591-1604.
- Yamaguchi, T. P., Bradley, A., McMahon, A. P. and Jones, S.** (1999a). A Wnt5a pathway underlies outgrowth of multiple structures in the vertebrate embryo. *Development* **126**, 1211-1223.
- Yamaguchi, T. P., Takada, S., Yoshikawa, Y., Wu, N. and McMahon, A. P.** (1999b). T (Brachyury) is a direct target of Wnt3a during paraxial mesoderm specification. *Genes Dev.* **13**, 3185-3190.
- Ybot-Gonzalez, P., Savery, D., Gerrelli, D., Signore, M., Mitchell, C. E., Faux, C. H., Greene, N. D. and Copp, A. J.** (2007). Convergent extension, planar-cell-polarity signalling and initiation of mouse neural tube closure. *Development* **134**, 789-799.
- Zhou, H., Kim, S., Ishii, S. and Boyer, T. G.** (2006). Mediator modulates Gli3-dependent Sonic hedgehog signaling. *Mol. Cell. Biol.* **26**, 8667-8682.
- Zhou, R., Bonneaud, N., Yuan, C. X., de Santa Barbara, P., Boizet, B., Schomber, T., Scherer, G., Roeder, R. G., Poulat, F. and Berta, P.** (2002). SOX9 interacts with a component of the human thyroid hormone receptor-associated protein complex. *Nucleic Acids Res.* **30**, 3245-3252.

Table S1. Primers used for quantitative RT-PCR

Gene	Forward (5'-3')	Reverse (5'-3')
<i>Bmp4</i>	AGATTGGCTCCCAAGAATCA	GCCTCCTAGCAGGACTTGG
<i>Dkk1</i>	CCGTCTGCCTCCGATCAT	GGACCAGAAGTGTCTTGCACAA
<i>Eomes</i>	CCACTGGATGAGGCAGGAGATTTC	AGTCTTGGAAGGTTCAATCAAGTCC
<i>Fgf5</i>	CGAGGAGTTTTTCAGCAACAA	CGCGGACGCATAGGTATTAT
<i>Gapdh</i>	TCAAGAAGGTGGTGAAGCAG	ACCACCCTGTTGCTGTAGCC
<i>Il2rg</i>	AATCCCCCATCAAGAATC	GTAGTCTGGCTGCAGACTCTCA
<i>Lef1</i>	AGCCTGTTTATCCCATCACG	TGAGGCTTCACGTGCATTAG
<i>Nanog</i>	CCTCCATTCTGAACCTGAGC	GCAATGGATGCTGGGATACT
<i>Nefl</i>	CCACTCTGCAAGCAAACAGA	CCACTGGATGAGGCAGGAGATTTC
<i>Nlgn3</i>	CTGTCTTTGGCTCTGGCATC	AGAGCCACTTTGGATGATGG
<i>Oct4</i>	AGCTGCTGAAGCAGAAGAGG	AGATGGTGGTCTGGCTGAAC
<i>Rest</i>	GTGCGAACTCACACAGGAGA	AAGAGGTTTAGGCCCGTTGT
<i>Rex1</i>	CCTGCACACAGAAGAAAGCA	CACTGATCCGCAAACACCT
<i>Sox2</i>	AGACCGTTTTTCGTGGTCTTG	TATCAACCTGCATGGGCATT
<i>T</i>	CAGCTGTCTGGGAGCCTGG	TGCTGCCTGTGAGTCATAAC